DOE/ET/53088-9 IFSR #9

DRIFT MODES IN AXISYMMETRIC TANDEM MIRRORS

Wendell Horton

Institute for Fusion Studies
The University of Texas at Austin
Austin, Texas 78712

February 1981

DRIFT MODES IN AXISYMMETRIC TANDEM MIRRORS

Wendell Horton

Institute for Fusion Studies
and the Department of Physics,
The University of Texas at Austin,
Austin, Texas 78712

Abstract

The drift mode analysis of the tandem mirror is developed for a large aspect ratio, axisymmetric model of the equilibrium. The axial drift wave eigenmodes are shown to change character as the plasma pressure varies with respect to the inverse aspect ratio. In the high beta regime the drift modes are transformed into a finite frequency convective cell and the flute-like ion drift wave. Quasi-linear formulae are given for the anomalous radial losses.

I. Introduction

A recent analysis[1] of low frequency drift modes in the tandem mirror system shows that there are two basic modes, an electron drift wave and a flute-like ion drift wave, that potentially lead to anomalous radial transport. Wave equations and the associated growth rates from particle resonances are derived in that work under the simplification that the axial wave functions are approximately sinusoidal standing modes with $k_{\parallel} = n\pi/L_c$, where L_c is the length of the central cell. In this article we investigate the axial eigenvalue problem for the electron and ion drift modes. We determine the turning points and conditions for localization as a function of plasma pressure from the axial wave equations.

The high beta equilibrium of the tandem mirror with quadrupole magnetic fields is sufficiently complicated that it is necessary to reduce the problem to a model equilibrium. The model used is that of an axisymmetric, long-thin equilibrium. Due to the large aspect ratio of the system the diamagnetic depression of the axial magnetic field dominates the effects from field line curvature in the equilibrium force balance equation. The axial variation of the magnetic field strength and the curvature of the field is calculated from the given on-axis vacuum magnetic field strength $B_o(z)$. Furthermore,

the central cell plasma is well approximated by local Maxwell-Boltzmann velocity distributions for each species, and hence the density and temperatures are constant along the magnetic field through the region of B_{max}. Here, $B_{max} = R_c B_c$ where B_c and R_c are the central cell magnetic field and mirror ratio, respectively. The dominant effects on the axial wave propagation are the variation of the magnitude of the magnetic field and the field line curvature. These equilibrium variations are shown to lead to turning points in the axial mode equations.

The basic parameters for the central cell plasma are (i) the plasma pressure $\beta = 8\pi p/B^2$, (ii) the aspect ratio L_c/r_n where L_c is the length of the central cell and r_n is the density gradient scale radius, and (iii) the radial gradient ρ_i/r_n where ρ_i is the thermal ion gyroradius. We define $\rho_i = c(m_i T_i)^{\frac{1}{2}}/eB$ and the cold ion inertial scale radius $\rho = \rho_i (T_e/T_i)^{\frac{1}{2}} = c_s/\omega_{ci}$. These parameters, and other drift wave related quantities, are given in Ref. 1 for the TMX device at Livermore. Tandem mirrors are characterized by $L_c/r_n \gtrsim r_n/\rho_i$ and $\beta < \beta_p < 1$ where β_p is the pressure of the plug plasma which provides the magnetohydrodynamic stability of the system. From the large aspect ratio condition $L_c/r_n > r_n/\rho_i$ it follows that (i) the azimuthal drift of the ions per longitudinal bounce is of order unity and (ii) the drift wave frequencies $\omega \sim \omega_*$ for the low order azimuthal modes $m = 1,2,3 \ldots$ exceed the ion transit

frequency $\omega_{ti} = v_i/L_c$. Following Ref. 1, we use a hydrodynamic description of the ions assuming $\omega > k_\parallel v_i \geq v_i/L_c$. We define two transitional values, β_1 and β_2, of the plasma pressure in terms of the aspect ratio: $\beta_1 = 8r_n^2/L_c^2$ and $\beta_2 = r_n/L_c$.

The magnetic field curvature in the solenoid is predominantly unfavorable with flute-interchange stability being provided by the plug plasma when $\beta < \beta_p$ as shown by Kaiser[2]. Thus, we investigate the conditions under which the unfavorable curvature in the solenoid may adversely affect the drift modes. For a sufficiently strong ion pressure gradient a short wavelength fluid-like drift mode occurs driven by the geometric mean of the local bad curvature and the ion pressure gradient. We estimate an anomalous ion thermal conductivity χ_i for this mode that scales like the resonant neoclassical plateau thermal conductivity[3]. For weaker pressure gradients the mode is more flute-like with the curvature producing a destabilizing frequency shift.

The electron drift wave for $\beta < \beta_1$ has a simple turning point due to the variation of the magnitude of B(s). At high pressures $\beta > \beta_2 = r_n/L_c$ the electron drift mode transforms into a slowly rotating convective cell.[4] The finite frequency and rotational velocity of the convective cell arises from the finite length and field line

curvature of the tandem mirror system. The linear convective cell is ion Landau damped; however, as Sagdeev, et al.[4] point out, the mode remains important due to the possibility of its providing anomalous transport when driven by parametric coupling to higher frequency unstable modes. The importance of convective cells as a mechanism for anomalous transport has also been pointed out by Dawson[5] in a different context. Two mechanisms for anomalous transport due to the drift modes are analyzed in Sec. IV. The conclusions are given Sec. V.

II. AXIAL EQUILIBRIUM MODEL

The equilibrium magnetic field is taken in the approximation of 1) azimuthal symmetry and 2) a small radius-to-length ratio. The magnetic field along the axis is taken to be $B_o(z)$ with a continuous second derivative. In some calculations, we use the model field profile

$$B_o(z) = B_c \hat{B}(z) \tag{1}$$

where, for example,

$$\hat{B}(z) = 1 + \frac{R_c - 1}{2}\left[\tanh\left(\frac{z - L_1}{\Delta L_1}\right) + 1\right] - \frac{\alpha(R_c - 1)}{2}\left[\tanh\left(\frac{z - L_2}{\Delta L_2}\right) + 1\right] . \tag{2}$$

The profile function $\hat{B}(z)$ describes the flat central cell field B_c for $z < L_1 - \Delta L_1$, the rise to the mirror field $B_{max} = R_c B_c$ for $z \simeq L_1 + \Delta L_1$, and the drop to the minimum plug field $R_c B_c (1 - \alpha) \approx R_c B_c/2$ at $z \simeq L_2 + \Delta L_2$.

The magnetic field $\underset{\sim}{B}(r,z)$ at the radius r in the central cell is related to the field on axis according to

$$B_r(r,z) = -\frac{r}{2}\frac{dB_o}{dz} , \tag{3}$$

$$B_z(r,z) = B_o(z) - \frac{r^2}{4}\frac{d^2B_o}{dz^2} - \frac{4\pi p(r)}{B_o(z)} . \tag{4}$$

The equation for the field line is $r^2 B_z(r,z) = \text{const}$, and the

axial magnetic flux function $2\pi\Psi \tilde{=} \pi r^2 B_z(r,z)$ is introduced as the radial coordinate.

The variation of the field strength as a function of the flux surface Ψ and the coordinate s along the field line is

$$B(\Psi,s) = B_o(s) - \frac{\Psi}{2}\frac{B_o''(s)}{B_o(s)} + \frac{3\Psi}{4}\left(\frac{B_o'(s)}{B_o(s)}\right)^2 - \frac{4\pi p(\Psi)}{B_o(s)} \quad . \tag{5}$$

Taking $\hat{b}$ as the unit tangent vector along the magnetic field line, it is straightforward to calculate the magnetic radius of curvature r_c given by

$$\hat{b}\times(\hat{b}\cdot\hat{\nabla})\hat{b} = \left(-\frac{rB_o''}{2B_o} + \frac{3}{4}\frac{rB_o'^2}{B_o^2}\right)\hat{e}_\theta = \frac{-\hat{e}_\theta}{r_c} \quad . \tag{6}$$

The curvature is unfavorable in the transition region where $B_o''/B > (3/2)\,(B_o'/B_o)^2$. This axial region $|z-L_1| \leqslant \Delta L_1 \approx L_t$, where the curvature is unfavorable ($r_c > 0$) produces a destabilizing shift in the frequencies of the drift modes.

The diamagnetic drift frequencies ω_{*j} associated with the azimuthal mode $\exp(im\theta)$ and the pressure gradient $dp_j/d\Psi$ are constant along the field line since

$$\omega_{*j} = \frac{k_\theta c}{e_j B n_j}\frac{dp_j}{dr} = \frac{mcT_j}{e_j}\frac{d\ell n p_j}{d\Psi} \quad , \tag{7}$$

where n_j and p_j are approximately independent of s outside of the plug plasma. Here, and in the following, the azimuthal wavenumber is $k_\theta = m/r$. The curvature drift frequency is

$$\omega_{Dj}(E,\mu) = -\frac{mc}{e_j}\frac{2(E-\mu B)}{r\hat{r}_c B} \quad , \tag{8}$$

and the grad-B drift frequency is

$$\omega_{\nabla Bj}(\mu) = \frac{mc\mu}{e_j}\frac{\partial B}{\partial \Psi} \simeq \frac{mc\mu}{e_j}\left[-\frac{1}{2}\frac{B_o''}{B_o} + \frac{3}{4}\left(\frac{B_o'}{B_o}\right)^2 - \frac{4\pi}{B_o}\frac{dp}{d\Psi}\right] \tag{9}$$

where for $\beta > \beta_1$, equilibrium pressure balance (5) and Eq. (7) give the last approximation. The Maxwell-Boltzmann averaged curvature drift frequency $\left\langle \omega_{Dj}(E,\mu) \right\rangle$ is

$$\left\langle \omega_{Dj} \right\rangle = -\frac{2mcT_j}{e_j r\hat{r}_c B} = \frac{2mcT_j}{e_j}\left(-\frac{B_o''}{2B_o^2} + \frac{3}{4}\frac{B_o'^2}{B_o^3}\right) \quad . \tag{10}$$

Henceforth we drop the averaging brackets on $\left\langle \omega_{Dj} \right\rangle$.

For flute-like axial modes it is the volume integral over the flux tube of the curvature drift frequency that enters the dispersion relation. Within the solenoid the flux tube-averaged drift frequency is always unfavorable since the weak-field region has a larger volume

$$\int_1^2 \frac{d\ell}{B}\omega_{Dj} = \frac{2mcT_j}{e_j}\left(-\frac{3}{4}\right)\int_{z_1}^{z_2} dz\, \frac{(B_0')^2}{B_0^4} \quad . \tag{11}$$

The flux tube averaged drift frequency is given by the $V''(\Psi)$ where $V'(\Psi)$ is the volume inside a vacuum flux tube given by

$$V' = \int_1^2 \frac{d\ell}{B} = \int_1^2 \frac{dz}{B_o - \frac{r^2}{4}B_o''} \cong \int_1^2 \frac{dz}{B_o}\left(1 + \frac{\Psi}{2}\frac{B_o''}{B_o}\right) = V_o' + \frac{3\Psi}{2}\int_{z_i}^{z_2} dz \left(\frac{B_o'}{B_o^2}\right)^2 \tag{12}$$

and, consequently,

$$V'' = \frac{3}{2}\int_{z_1}^{z_2} dz\left(\frac{B_o'}{B_o^2}\right)^2 \quad . \tag{13}$$

Thus, from Eqs. (11) and (13) the flux tube averaged curvature drift frequency $\bar{\omega}_{Dj}$ is

$$\bar{\omega}_{Dj} = -\frac{mcT_j V''}{e_j V'} \quad , \tag{14}$$

and

$$\omega_{*j}\,\bar{\omega}_{Dj} = -\left(\frac{mcT_j}{e_j}\right)^2 \frac{d\ell n p_j}{d\Psi}\,\frac{d\ell n V'}{d\Psi} > 0$$

for $p_j'(\Psi) < 0$. We use Eqs. (10), (13), and (14) to define the flux tube-averaged radius of curvature $\bar{r}_c$ which is given by $\bar{r}_c = 2V'/rBV''$ and is of order $L_t L_c/r$ and unfavorable for the solenoid.

An example of the axial variation of the magnetic field and the curvature parameter is shown in Fig. 1. The plasma diamagnetism increases the strength of the unfavorable curvature $\varepsilon_n(s)$ over the vacuum value shown in Fig. 1 and calculated from Eq. (6). The effect is not substantial, however, and is neglected in the present work.

III. High Pressure Drift Modes

In the hydrodynamic approximation for the cross-field currents the condition of force balance on the Alfven time scale leads to the diamagnetic depression $\delta B_\parallel$ due to the convected plasma pressure fluctuation δp. Since the drift modes have $\omega_k << k_\perp v_A$ it follows that $B\delta B_\parallel + 4\pi\delta p_\perp = 0$ as derived in Ref. 1, Sec. 4 and Ref. 6, Chap. 13. For both the ion and the electron drift modes the magnetic fluctuation is substantial with $\delta B_\parallel / B \simeq \beta(e\phi/T_e)$. The effect of $\delta B_\parallel$ within the hydrodynamic theory for the cross field charge separation $\nabla_\perp \cdot \delta \underset{\sim}{j}_\perp$ is to reduce the contribution that arises from the $p_\perp \nabla_\perp B$ drifts and the diamagnetic current to a term proportional to $\delta p_\perp / r_c$. Without repeating the analysis of Ref. 1 here, we give the principal result for the net charge separation from the magnetic drifts

$$\nabla_\perp \cdot \delta \underset{\sim}{j}_\perp = - \frac{i2mc\delta p}{r r_c B} ,$$

where δp is the total perturbation in the plasma pressure and r_c is the radius of curvature of the vacuum magnetic field

The magnetic oscillations and the inductive component of the parallel electric field are given by $\delta \underset{\sim}{B}_\perp = \nabla \times (A_\parallel \hat{b}) = \nabla_\perp A_\parallel \times \hat{b}$ and $E_\parallel^{(A)} = i\omega A_\parallel / c = d\psi/ds$. With both ϕ and ψ normalized to T_e/e, we obtain the equations

$$b_x = \frac{\delta B_x}{B} = i\frac{k_\theta}{B} A_\parallel = \frac{\omega_{*e}}{\omega} r_n \frac{d\psi}{ds} , \tag{15}$$

$$\frac{r_n e E_\parallel}{T_e} = -r_n \frac{d}{ds}(\phi - \psi) , \tag{16}$$

$$\frac{j_{\parallel}}{en_e c_s} = -\frac{i2k_\theta \rho}{\beta_e} b_x \quad , \tag{17}$$

for the normalized fluctuating fields and current density. We use the well-known formula for the parallel conductivity derived in Ref.1, Sec. 3.1 and Ref. 6, Chap. 12.

Neglecting the weak parallel compression from $\gamma p_i \nabla_{\parallel} v_{\parallel}$, thermal balance for the ions gives the convective transport of the ion pressure

$$\frac{\delta p_i}{p_i} = -\frac{\omega_{*i}}{\omega}\left(\frac{e_i \phi}{T_i}\right) .$$

The perturbed electron pressure is readily computed from either δf_e in Eq. (42) of Ref. 1 or from the electron fluid equations with $\underset{\sim}{B}\cdot\nabla T_e \simeq 0$, in Sec. 2.3 of Ref. 1. We obtain that

$$\frac{\delta p_e}{p_e} = \frac{e\phi}{T_e} - \left(1 - \frac{\omega_{*e}}{\omega}\right)\left(\frac{e\psi}{T_e}\right) - \left(1 - \frac{\bar{\omega}_{*e}}{\omega}\right)\hat{\mathcal{L}}\left(\frac{e\phi}{T_e} - \frac{e\psi}{T_e}\right)$$

where $\hat{\mathcal{L}}$ is the electron bounce averaging operator defined in Appendix A. Evidently, the total plasma pressure fluctuation can be written as

$$\delta p = p_e\left[\left(1 - \frac{\omega_{*i}}{\omega}\right)\phi - \left(1 - \frac{\omega_{*e}}{\omega}\right)\left(\psi - \hat{\mathcal{L}}\psi + \hat{\mathcal{L}}\phi\right)\right] \tag{18}$$

where ϕ and ψ are measured in units of T_e/e.

Taking into account the divergence of the finite ion inertia currents and expressing the divergence of the parallel plasma current in terms of ψ, we obtain equations that correspond to Eqs. (47) and (48) in Ref. 1 for $\phi(s)$ and $\psi(s)$. The present equations contain an improved description of the charge separation produced by the field-line curvature.

With the approximation that $\nabla_\perp^2\phi = -k_\theta^2\phi$ the equations governing $\psi(s)$ and $\phi(s)$ are

$$B\frac{d}{ds}\left(\frac{(k_\theta\rho)^2 v_A^2}{B}\frac{d\psi}{ds}\right) + \left[(k_\theta\rho)^2\omega(\omega-\omega_{*i}) + 2\varepsilon_n\omega_{*e}(\omega-\omega_{*i})\right]\phi$$

$$- 2\varepsilon_n\omega_{*e}(\omega-\omega_{*e})(\psi - \hat{\mathcal{L}}\psi + \hat{\mathcal{L}}\phi) = 0 \qquad (19)$$

$$B\frac{d}{ds}\left(\frac{(k_\theta\rho)^2 v_A^2}{B}\frac{d\psi}{ds}\right) + \left[\omega(\omega-\omega_{ne})(1-\hat{\mathcal{L}}) + \left(1-\frac{\omega_{*i}}{\omega}\right)c_s^2 B\frac{d}{ds}\frac{1}{B}\frac{d}{ds}\right](\psi-\phi) = 0 \qquad (20)$$

In deriving Eqs. (19) and (20) we rewrite the drift term according to $(T_e/T_i)(\omega_{Di}(s)/\omega) = -2k_0\varepsilon_n(s)/\hat{\omega}$ where $\varepsilon_n(s) = r_n/r_c(s)$ and is positive in the region of unfavorable curvature. Here, we do not consider the rotational or interchange instabilities of Refs. 7 and 2.

Analysis of the local dispersion relation obtained by replacing $\hat{b}\cdot\nabla \sim ik_\parallel$ with $k_\parallel = n\pi/L_c$ shows that there are two regimes. The regimes are a function of β compared to the inverse aspect ratio r_n/L_c. In the lower plasma pressure regime we calculate $\psi(s)$ perturbatively from the lowest order solutions $\phi_0(s)$, ω_o given in Sec. III-A. At high plasma pressure, the parallel current equation requires that $\psi(s) = \phi(s) + \delta\psi(s)$ where we now calculate $\delta\psi(s)$ perturbatively. For intermediate pressure $\beta_1 < \beta < \beta_2$, the equations for ϕ and ψ are strongly coupled.

A. Low Pressure Mode Equations

First we consider the axial eigenvalue problem in the low pressure regime. From Eq. (20) it follows that the fluctuating field ψ is small compared with the potential ϕ when

$$(k_\perp \rho)^2 \, k_\parallel^2 v_A^2 \gg \omega(\omega-\omega_{ne}) \quad ,$$

which for $0 \leq \omega \leq \omega_{ne}$ and $k_\parallel L_c \sim 1$ leads to the critical plasma pressure β_1 given by

$$\beta_1 = \frac{8r_n^2}{L_c^2} \quad . \tag{21}$$

For $\beta > \beta_1$ modes at $\omega \sim \omega_{ne}/2$ become electromagnetic. Modes with $\omega \sim 0$ or $\omega \sim \omega_{ne}$ may remain electrostatic, however.

For low plasma pressure, $\beta < \beta_1$, we write $\phi(s) \cong \phi_0(s)$ and compute $\psi(s)$ perturbatively. The axial mode equations (19) and (20) are subtracted and ψ is ignored compared with ϕ to obtain

$$B\frac{d}{ds}\left(\frac{1}{B}\frac{d\phi_0}{ds}\right) + \frac{\omega^2}{c_s^2}\left[(k_\perp\rho)^2 + \frac{2\varepsilon_n(s)\omega_{ne}}{\omega} + \left(\frac{\omega-\omega_{ne}}{\omega-\omega_{*i}}\right)(1-\hat{\mathcal{L}}-i\delta\hat{\mathcal{L}})\right]\phi_0(s)=0, \tag{22}$$

while Eq. (20) gives

$$B\frac{d}{ds}\left[\frac{(k_\theta\rho)^2 v_A^2}{B(s)}\frac{d\psi}{ds}\right] = \left[\omega(\omega-\omega_{ne})(1-\hat{\mathcal{L}}) + (1-\frac{\omega_{*i}}{\omega})c_s^2 \, B\frac{d}{ds}\frac{1}{B}\frac{d}{ds}\right]\phi_0(s) \quad . \tag{23}$$

As given in Appendix A, the operator $\hat{\mathcal{L}}\phi = \langle\bar{\phi}\rangle_{M-B}$ is the Maxwell-Boltzmann velocity average of the bounce averaged potential $\bar{\phi}$, and the operator $i\delta\hat{\mathcal{L}}\phi$ contains the resonant wave-electron interactions. The resonant contri-

bution is treated perturbatively since its value depends on the shape of the wave function.

On the flux surface the axial variation of $(k_\perp \rho)^2$ is given by

$$(k_\perp \rho)^2 = \frac{k_0^2 B_c}{B(s)} ,$$

where we introduce the dimensionless variables $k_0 = k_\theta \rho$ with ρ defined by the values of r and B_c in the central cell. We define $\hat{\omega} = \omega r_n / c_s$ with the constant r_n defined in the uniform region of the central cell.

Equation (22) has turning points in the high magnetic field region for modes with frequencies such that $0 \leq \omega < \omega_{ne} = k_o$ due to the increase in $\hat{B}(s)$ and due to $\varepsilon_n(s)$. An example of the local parallel wavenumber $k_\parallel(\omega, k_0, \eta_i, \varepsilon_n, s)$ is shown in Fig. 2 for typical values of the parameters. The maximum of $k_\parallel(s)$ corresponds to the maximum of the unfavorable curvature. This maximum and the turning point in the high field region are the important features of $k_\parallel(\omega, k_0, s)$.

For weak ion pressure gradients the eigenmode is given approximately by

$$\phi_0(z) = \left(\frac{\Phi_0 z}{L_\phi}\right) \exp\left(-\frac{z^2}{2L_\phi^2}\right) \qquad (24)$$

with

$$L_\phi = \left(\frac{c_s}{\omega} \quad \frac{L_B}{k_o} \right)^{\frac{1}{2}} , \tag{25}$$

where $L_B \sim L_t$ is the characteristic scale length for variation of the magnetic field strength B(s). The dispersion relation for mode (24) is

$$\frac{\hat{\omega}-k_0}{\hat{\omega}+k_0(1+\eta_i)} + k_0^2 - \frac{3r_n k_0}{L_B \hat{\omega}} = 0 \tag{26}$$

with $\phi(z)$ localized to the region $z \lesssim L_B$ when the last term in Eq. (26) is subdominant. In this regime $k_0 \gtrsim (r_n/L_B)^{\frac{1}{2}}$ the frequency of the electron drift wave is

$$\hat{\omega}(k_0) \cong \frac{k_0\left[1-k_0^2(1+\eta_i)\right]}{1+k_0^2} . \tag{27}$$

The growth rate γ_k follows from the wave function (24), the frequency (27) and the relevant form of the electron dissipation as given by

$$\frac{\gamma_k \omega_{*e}}{\omega_k^2} = \int_{-\infty}^{+\infty} \frac{dz}{B(z)} \phi_0^*(z) \hat{\delta\mathcal{L}} \phi_0(z) \left(\int_{-\infty}^{+\infty} \frac{dz\,|\phi_0|^2}{B(z)} \right)^{-1} . \tag{28}$$

where $\hat{\delta\mathcal{L}}$ is given in Appendix A for the tandem mirror system.

For large values of the ion pressure gradient a ballooning drift mode occurs that is driven by the local bad curvature and the ion pressure gradient. To obtain the approximate form of this ballooning drift mode we approximate

the maximum of $\varepsilon_n(z)$ by $\varepsilon_n[1-(z-z_m)^2/L_\varepsilon^2]$ where $z_m \simeq L_1$ and $L_\varepsilon \simeq L_t \simeq 2\Delta L_1$ according to formulae (1), (2), and (6). The eigenmode is now approximately

$$\phi_0(z) = \Phi_0 \exp\left[-\frac{(z-z_m)^2}{2L_\phi^2}\right] \tag{29}$$

valid for $L_\phi \lesssim L_1$, with the recognition that $\varphi(z=0)\approx 0$ and $\varphi(-z) = -\varphi(z)$. The dispersion relation for mode (29) is readily obtained and solved for $\omega(k_0)$ to find that

$$\hat{\omega}(k_0) = \frac{k_0}{2(1+k_0^2)}\left\{u_{k_0} \pm [u_{k_0}^2 - 8\varepsilon_n(1+\eta_i)(1+k_0^2)]^{\frac{1}{2}}\right\}, \tag{30}$$

where $u_{k_0} = 1-2\varepsilon_n - k_0^2(1+\eta_i)$. The maximum value of ε_n according to Eq. (6) is $\varepsilon_n \simeq r_n r/L_t^2$ which is small compared with unity. For u_{k_0} of order unity there are two real modes: 1) the electron drift wave, $\hat{\omega}_+(k_0) \simeq k_0 u(k_0)/(1+k_0^2)$, modified by the ion pressure gradient and the field curvature and 2) the slow mode, $\hat{\omega}_- \simeq k_0 2\varepsilon_n(1+\eta_i)/u(k_0)$, due to the pressure gradient and the curvature. For azimuthal wavenumbers centered about $k_0 \simeq (1+\eta_i)^{-\frac{1}{2}}$, the dispersion relation (30) gives an unstable fluid-like mode with a growth rate that exceeds the wave frequency. The growth rate is given by

$$\hat{\gamma}(k_0) \cong \frac{k_0\left[2\varepsilon_n(1+\eta_i)\right]^{1/2}}{(1+k_0^2)^{\frac{1}{2}}} \lesssim [2\varepsilon_n(1+\eta_i)]^{\frac{1}{2}}, \tag{31}$$

which, in dimensional form and with the approximation $\varepsilon_n \sim (r_n/L_t)^2$, yields $\gamma \sim (c_s/L_t)(1+\eta_i)^{\frac{1}{2}}$.

The growth rate exceeds the ion transit frequency when $\eta_i \gtrsim 1$. The pressure gradient driven mode rotates in the ion diamagnetic drift direction and has a growth rate that is similar to the ballooning interchange mode[2] except that it occurs for azimuthal wavelengths on the scale of, but several times greater than, the ion gyroradius.

The approximate width of the modes with $k_0 \sim 1$ is

$$L_\phi \simeq \frac{(r_n L_t)^{\frac{1}{2}}}{(2\varepsilon_n)^{3/8}(1+\eta_i)^{1/8}}$$

which is comparable to L_t for the parameters of interest ($\varepsilon_n \sim r r_n / L_t^2$). The onset of trapping of the wave function is investigated in Appendix B.

An example of the wave function obtained from integrating Eq. 22) with the model magnetic field profile given in Fig. 1 is shown in Fig. 2. For $k_o = 0.6$ and $\eta_i = 1.0$ the solution of the eigenvalue problem (22) yields $\omega r_n/c_s = 0.391$ which is consistent with Eq. (26) and gives $\omega_k/\omega_{*e} \sim 2/3$. For the same k_o and η_i the complex eigenvalue given approximately by Eq. (30) is also found with $\omega r_n/c_s = -0.101 + i\,0.295$. For comparison the growth rate given by Eq. (31) is $\gamma r_n/c_s = 0.29$ using $2\varepsilon_n = 0.16$. In most integrations the wave function is small, but perhaps not negligible, in the region of the plug plasma. The effect of the plug plasma on the central cell drift waves, while noted in Sec. 4.2 of Ref. 1, requires further investigation.

B. High Pressure Mode Equations

Now, we consider the approximate solution of the axial mode equation when $\beta >> \beta_1$. In this regime the oscillating parallel electron current is large except at a frequency sufficiently close to ω_{ne} or for a sufficiently flute-like wave function. Excluding these two exceptional conditions ($\omega \neq \omega_{ne}$ and $\phi \neq$ const) the parallel current Eq. (20) may be solved perturbatively to obtain, with $\Omega = \omega/\omega_{ne}$,

$$\psi(s) = \phi_0(s) - \frac{2r_n^2(1-\hat{\mathcal{L}})^{-1}}{\beta\Omega(\Omega-1)} \frac{d^2\phi_0}{ds^2} \quad , \tag{32}$$

which determines the parallel electric field

$$\frac{r_n eE_\parallel}{T_e} = \frac{-2r_n^3}{\beta\Omega(\Omega-1)} \frac{d^3\phi_0}{ds^3} \sim \frac{\beta_1}{\beta} \frac{r_n}{L_c} \phi_0 \tag{33}$$

from Eqs. (16) and (32) assuming that $\|\hat{\mathcal{L}}\phi_0''\| << \|\phi_0''\|$. The lowest order eigenfunction and eigenvalue now follow from Eq. (19) with $\psi(s) = \phi_0(s)$.

The axial mode equation in the regime $\beta >> \beta_1$ is, from Eqs. (19) and (32),

$$B \frac{d}{ds}\left[\frac{(k_\theta\rho)^2 v_A^2}{B} \frac{d\phi_0}{ds}\right] + \left[(k_\theta\rho)^2\omega(\omega-\omega_{*i}) + 2\varepsilon_n\omega_{*e}(\omega_{*e}-\omega_{*i})\right]\phi_0 = 0 \quad , \tag{34}$$

where $\omega_{*e} - \omega_{*i}$ is proportional to the total plasma pressure gradient. In this high pressure regime $\beta >> \beta_1$ the mode equation is the finite-Larmor-radius fluid equation even though $\omega << \omega_{be}$, provided $\|\hat{\mathcal{L}}\phi_0''\| < \|\phi_0''\|$ so that the correction term

in Eq. (32) is bounded by β_1/β .

To analyze Eq. (34) in the drift mode regime, it is again convenient to use the dimensionless frequency and wave-number $\hat{\omega}=\omega r_n/c_s$ and $k_0=k_\theta \rho$, defined at the miplane of the central cell. In terms of these dimensionless variables we observe that

$$\gamma^2_{mhd}(s) \equiv \frac{2\varepsilon_n(s)\omega_{*e}(\omega_{*e}-\omega_{*i})}{(k_\theta\rho)^2}$$

$$= 2\varepsilon_n(s)\left[1+\eta_e+\frac{T_i}{T_e}(1+\eta_i)\right], \qquad (35)$$

and the mode equation becomes

$$2r_n^2\hat{B}(s)\frac{d}{ds}\left[\frac{1}{\hat{B}(s)}\frac{d\phi_0}{ds}\right]+\beta_e\left\{\hat{\omega}\left[\hat{\omega}+k_0(1+\eta_i)\right]+\gamma^2_{MHD}(s)\right\}\phi_0=0 \qquad (36)$$

This is an elementary form of the magnetohydrodynamic-ballooning mode equation obtained by Kaiser with eikonal approximation and minimization of the action density.[2] In terms of his variables we have the case where $p_\perp=p_\parallel$, $S_\alpha=k_\theta$, $S_\psi=0$, and $K_\psi=-1/r_c(s)$ and $V(\ell)=\phi_0(s=\ell)$. Here, we recall that Kaiser finds that the most unstable perturbations occur for $S_\psi=k_r=0$ on the field line along the symmetry planes. For the plug plasma pressure less than $\beta_p < 1/3$ to $1/2$ the magnetohydrodynamic ballooning from the unfavorable curvature in the solenoid limits the solenoid plasma pressure to $\beta<\beta_p$. We do not consider further the magnetogydrodynamic stability problem and assume that β is below the magnetohydrodynamic limit.

The variation of $\varepsilon_n(s)$ in Eq. (36) occurs on the scale L_t and induces a variation in $\phi(s)$ on the scale

$$L_\phi = \frac{(r_n L_t)^{1/2}}{(\beta\varepsilon_n)^{1/4}} \quad , \tag{37}$$

which becomes comparable to L_t when

$$\beta \sim \frac{r_n r_c}{L_t^2} \sim \frac{r_n}{r} \sim 1.$$

Thus, for $\beta<\beta_p<1$ the modes are only weakly ballooning in the bad curvature region. These flute-like modes are marginally stable oscillations which have $L_\phi \lesssim L_c$. The two oscillation branches of Eq. (34) are the ion flute mode $\omega \simeq \omega_{*i}$ and the low frequency limit of the electron drift wave $\omega \simeq -k_\parallel^2 v_A^2/\omega_{*i}$ which is the convective cell of Sagdeev et al.[4] in the limit $k_\parallel = 0$.

Calculating the dispersion relation for these flute-like modes perturbatively we obtain the finite beta ion diamagnetic drift mode given by

$$\omega_1(k_0) = -k_0(1+\eta_i) + \frac{2\bar{\varepsilon}_n}{k_0(1+\eta_i)} - \frac{2r_n^2}{\beta L_c^2 k_0(1+\eta_i)} \quad , \tag{38}$$

where $\bar{\varepsilon}_n > 0$ is defined using the average curvature introduced in Sec. II. The frequency shift from the curvature is unfavorable with respect to ion Landau resonances and dominates the favorable shift from line bending when $\beta\bar{\varepsilon}_n > \beta_1/8$ or $\beta > L_t/L_c$.

The second marginally stable oscillation given by Eq. (34) rotates slowly in the electron direction and connects to the electron drift wave when $\beta \sim \beta_1$. The mode is the low frequency convective cell or the magnetohydrodynamic roll of Sagdeev, et al.[4], with a frequency

$$\omega_2(k_0) = \frac{-2\bar{\varepsilon}_n}{k_0(1+\eta_i)} + \frac{2r_n^2}{\beta L_c^2 k_0(1+\eta_i)} \qquad (39)$$

determined by the finite geometry of the tandem mirror system. Due to the low frequency of the convective cell the condition for $\psi(s) = \phi_0(s) + \delta\psi(s)$ in Eq. (32) must be re-examined. It is found that for $\beta_1 \lesssim \beta \lesssim \beta_2 = r_n/L_c$ the small $\delta\psi$ approximation fails and the coupled set of second order differential equations, Eqs. (19) and (20), must be solved. For $\beta > r_n/L_c$, however, the parallel ion current dominates the electron current and the small $\delta\psi$ approximation becomes valid with $|\delta\psi|/|\phi_0| \sim (r_n/\beta L_c)^2$. For the ion drift mode no such gap in the β/β_1 expansion occurs.

In the laboratory reference frame with $E_r \simeq T_e/er$ both modes $\omega_1(k_0)$ and $\omega_2(k_0)$ rotate in the ion diamagnetic direction. We do not consider modes due to centrifugal acceleration or sheared rotation in this work.

Modeling the even mode field by $\phi(s) = \Phi_0 \exp(-s^2/2L_\phi^2)$ we obtain

$$b_x = \frac{i\Phi_0 r_n s}{\Omega L_\phi^2 \hat{B}(s)} \exp(-s^2/2L_\phi^2) \quad ,$$

$$\frac{j_\parallel}{enc_s} = \frac{2i\Phi_0 k_0 r_n s}{\Omega \beta_e L_\phi^2 \hat{B}(s)} \exp(-s^2/2L_\phi^2) \quad ,$$

and from Eq. (33)

$$\frac{er_n E_\parallel}{T_e} \simeq \frac{2r_n^3 \Phi_0 s(s^2/L_\phi^2 - 3)}{\beta\Omega(\Omega-1)L_\phi^4} \exp\left(-\frac{s^2}{2L_\phi^2}\right).$$

For $k_o=0.6$, $\eta_i=1$ and $\beta=0.3$ the local parallel wavenumber and the solution of the high beta eigenvalue problem are shown in Fig. 3. The two eigenfrequencies corresponding to the approxiamte frequencies in Eq. (38) and (39) are found to be $\omega_1 r_n/c_s = -1.11$ and $\omega_2 r_n/c_s = -0.0867$.

Rosenbluth[11] has recently pointed out that in addition to the even mode with $L_\phi \sim L_c$ there is a strict flute solution for which the eigenvalue λ of the operator $\hat{\mathcal{L}}$ is unity and $E_\parallel$ from Eq. (16) vanishes since ϕ and ψ are constant along the flux tube. For the flute mode the pressure fluctuation (18) is identical to that given by the magnetohydrodynamic equations, and the dispersion relation is the finite Larmor radius interchange equation.

C. Intermediate Pressure Regime

There is an intermediate plasma pressure range approximately between β_1 and β_2 in which the coupled differential Eqs. (19) and (20) must be used to describe the plasma eigenmodes. Solving the axial eigenvalue problem in this intermediate regime is a complicated study that requires further work. Some basic features of the transitional regime can be understood from a local analysis of the coupled equations. Here we consider briefly the results of the local analysis.

We consider that the axial modes governed by Eqs. (19) and (20) balloon sufficiently in the regions of bad curvature $\varepsilon_n(s) > 0$ that the function $\varepsilon_n(s)$ may be characterized by a given positive value. We furthermore assume that the parallel differential operators can be characterized by the value $k_\parallel$ such that $k_n r_n = r_n/L_c = \varepsilon$. With these approximations we define the characteristic Alfven frequency as $\omega_A = (2/\beta)^{1/2}\varepsilon$ and the ion-acoustic frequency as $\omega_s = \varepsilon$, recalling that frequencies are measured in units of c_s/r_n. We also define the low pressure growth rate in Eq.(31) as $\gamma_{es} = [2\varepsilon_n(1 + \eta_i)]^{1/2}$ and recall the high pressure growth rate is given in Eq. (35) by $\gamma_{mhd} = [2\varepsilon_n(2 + \eta_i + \eta_e)]^{1/2}$ for $T_i = T_e$. With these considerations we reduce Eqs.(19) and (20) to a dispersion relation which is a fifth order polynomial with real coefficients. We have analyzed the polynomial on the low and high pressure regimes to recover the local approximations to the eigenmodes obtained in

the preceeding subsections A and B. Now we analyze the intermediate regime numerically.

In Fig. 5 the frequency and growth rate versus aximuthal wavenumber k are shown for a plasma pressure just below and just above the onset of the magnetohydrodynamic modes. In Fig. 5a below the onset the plasma pressure is $\beta = 0.02$ where $\omega_A = 1.0$ and $\omega_s = \varepsilon = 0.1$. The two Alfven oscillations are the higher frequency branches in the figure and the three lower oscillations are approximately electrostatic in polarization with $|\psi/\phi| \lesssim \frac{1}{2}$. The unstable branch is described approximately by Eq. (30) with the maximum growth rate occurring at finite k. Increasing the plasma pressure to $\beta = 0.05$ the prarmeters change to $\omega_A = 0.632$ and $\omega_s = \varepsilon = 0.1$ with $\gamma_{mhd} \gtrsim \omega_A$.

The numerical solution given in Fig. 5b shows that the unstable branch now has a maximum growth rate near $k = 0$ and is polarized such that $|\psi/\phi - 1| \lesssim \frac{1}{2}$ with $\psi/\phi \to 1$ as beta increases further. The other frequencies in Fig. 5b are the electromagnetic drift wave with $\omega \simeq k$ and $|\psi/\phi| > \frac{3}{2}$ and the unstable ion-acoustic like mode with $\omega \simeq -2k\varepsilon_n$ and $\gamma_s = \pm \omega_s(1 + \eta_i)^{1/2}$.

Analysis of the fifth order polynomial dispersion relation in the transitional regime discussed in Fig. 5 shows that the maximum growth rate occurs at approximately

$$k_m = \frac{(1 - 2\varepsilon_n - \gamma_{mhd}^2/\omega_A^2)^{1/2}}{(1 + \eta_i)^{1/2}} \quad .$$

For $\gamma_{mhd}^2 < \omega_A^2$ the maximum growth rate is approximately γ_{es} at $k_m \lesssim (1 + \eta_i)^{-1/2}$ and for $\gamma_{mhd}^2 > \omega_A^2$ the maximum growth rate is γ_{mhd} occurring at the smallest allowed value of k consistent with the discrete azimuthal mode numbers and the condition $k_\theta \geqslant k_r$ from the local radial theory.

Before turning to the quasilinear transport formulae in the next section we note that the mode coupling estimate for the magnitude[9,10] of the fluctuating fields is given by $\Phi_0 \simeq A\rho/r_n$ where A is of order unity and is a function of the dimensionless parameters $\beta, \eta_i, \eta_e, T_e/T_i$ and k_0. The radial distribution of ρ/r_n is given in Figs. 1 and 2 of Ref. 1 for two model profiles.

IV. ANOMALOUS TRANSPORT FORMULAS

Due to the discreteness of the azimuthal mode spectrum for $k_\perp \rho_i < 1$, we divide the wave-induced transport problem into two regimes: 1) where the frequency spectrum has sharp lines at the eigenfrequencies and their harmonics and 2) where there is a broad band of frequencies described by the correlation time $\tau_c = 1/\Delta\omega_k$. The regime may be determined from fluctuation measurements rather than ab initio. In the presence of sharp frequency lines at ω_{k_o} the losses are calculated from the guiding center motion in the asymmetric electric and magnetic fields. The calculation follows that of the particle losses by Kishinevskij, et al.[3], particularly for the losses in the Stochastic Electron Mirror, where now the amplitudes ϕ_{k_o} and ψ_{k_o} play the role of their asymmetry parameter α. Here, we consider the quasilinear regime and report later on the resonant and stochastic guiding center losses.

For a spectrum of low frequency fluctuations quasilinear theory applies when the amplitude and the correlation time of the turbulence is such that both the E×B and $E_\parallel$ trapping of the guiding center motion is weak. The conditions are

$$R_{E\times B} = \langle \omega_{b_\perp}^2 \tau_c^2 \rangle = \sum_{\underset{\sim}{k}} \frac{c^2 k_x^2 k_y^2 |\phi_{\underset{\sim}{k}}|^2}{B^2 [\Delta(\omega_{\underset{\sim}{k}} - k_\parallel v_\parallel)]^2} < 1 \quad ,$$

and

$$R_{E_\parallel} = \langle \omega_{b_\parallel}^4 \tau_c^4 \rangle = \sum_{\underset{\sim}{k}} \left(\frac{e}{m}\right)^2 \frac{k_\parallel^4 |\phi_{\underset{\sim}{k}} - \psi_{\underset{\sim}{k}}|^2}{[\Delta(\omega_{\underset{\sim}{k}} - k_\parallel v_\parallel)]^4} < 1 \quad .$$

For the spectra due to the modes in Sec. III we estimate that the nonlinearities are due to the ions with $R^i_{E\times B} >> R^e_{E_\parallel}$. We have $R^i_{E\times B} \sim 1$ at $e\phi_o/T \sim 1/\bar{k}_x r_n$ where $\bar{k}_x$ is the mean radial wavenumber in the fluctuation spectrum. At this level a spectrum with $k_\perp \rho \sim 1$ and $k_\parallel r_n \sim r_n/L_c \sim \rho/r_n$ has $R^e_E < 1$ for the resonant electrons provided $\rho/r_n \lesssim (m_e/m_i)^{1/3}$. Recently, Nevins[8] has pointed out that the condition $R^e_E < 1$ may not be satisfied for the TMX parameters.

The fluctuating electric and magnetic fields give rise to net radial transport of particles and thermal energy. The magnitude of the transport is proportional to the intensity of the fluctuations and the phase correlation between the particle and the electromagnetic fields. The net particle transport follows from the space-time average of the azimuthal component of momentum balance

$$\left\langle \tilde{n}_j \tilde{E}_\theta + \frac{1}{c} \tilde{\Gamma}_j \times \tilde{B} \right\rangle - \frac{1}{c} \Gamma_j B = - \frac{m_j}{e_j} \int v_\theta C(f_j) dv \quad , \tag{40}$$

where $m_j \int v_\theta C_j dv$ is the collisional rate of change of momentum and $\langle \ldots \rangle$ is the θ, t average of the fluctuating fields.

For the modes considered in Sec. III the average force on the ions and the electrons reduces to

$$\Gamma_i = \frac{c}{B} \left\langle \tilde{n}_i \tilde{E}_\theta \right\rangle = \frac{c}{B} \sum_{k_\theta} i k_\theta \phi^*_k(s) n_k(s) \quad , \tag{41}$$

$$\Gamma_e = \frac{c}{B} \left\langle \tilde{n}_e \tilde{E}_\theta + \frac{1}{c} \Gamma_{e\parallel} \delta \tilde{B}_x \right\rangle$$

$$= \frac{c}{B} \sum_{k_\theta} i k_\theta \left[\phi^*_k(s) n_{ek}(s) + \frac{1}{ec} A^*_{\parallel k}(s) j_{\parallel e}(s) \right] \quad , \tag{42}$$

so that only the out-of-phase or dissipative components of n_k, ϕ_k and $j_{\parallel k}$, $A_{\parallel k}$ contribute.

In the case of a local dissipative contribution $i\delta_j(k_\theta,s)$ to the particle response, the formulae become

$$\Gamma_i(s) = \frac{n_e c T_e}{eB} \sum_{k_\theta} k_\theta \delta_i(k_\theta,s) \left| \frac{e\phi_k(s)}{T_e} \right|^2 , \tag{43}$$

$$\Gamma_e(s) = \frac{n_e c T_e}{eB} \sum_{k_\theta} k_\theta \delta_e(k_\theta,s) \left| \frac{e\phi_k(s)}{T_e} - \frac{e\psi_k(s)}{T_e} \right|^2 , \tag{44}$$

where $\delta_j(-k_\theta) = -\delta_j(k_\theta)$ is the dissipative part of the particle propagator, $\delta_j = -\mathrm{Im}\langle g_k^j(E,\mu,s)\rangle$, averaged over the Maxwell-Boltzmann velocity distribution.

In the case where the electron response is through the bounce averaged electromagnetic fields, it is only convenient to compute the flux tube volume integral of the radial flux. Integrating the θ,t averaged force over the flux tube volume yields

$$\Gamma_e = \frac{-n_e c T_e}{e\langle B\rangle} \sum_{k_\theta,k_\parallel} \int_0^\infty dE \int_0^\infty d\mu \tau F_e^M(E) k_\theta (\omega_k - \omega_{*e}) \times \sum_{n=-\infty}^{+\infty} \pi\delta(\omega_k - n\omega_b) J_n^2(k_\parallel s_0) \left| \phi_{k_\theta,k_\parallel} - \psi_{k_\theta,k_\parallel} \right|^2 , \tag{45}$$

where $\langle B\rangle = \int_1^2 ds / \int_1^2 ds/B(s)$. In obtaining Eq. (45) we performed the orbit integration by first writing $\phi(s)$, $\psi(s) = \sum_{k_\parallel} \left(\phi_{k_\parallel}, \psi_{k_\parallel}\right) \exp(ik_\parallel s)$ and then making a sinusoidal orbit approximation for the bounce motion of the electrons.

Let us consider the case of the electron drift wave where ω_k is well below ω_{ne} due to the k_0^2, η_i and ε_n frequency shifts. Depending on the value of these parameters the frequency ω_k is given by Eq.(27) or Eq.(30). The first harmonic resonance occurs with $\omega_k = \omega_b(v_\parallel, v_\perp) \simeq v_\parallel / L_c$.

We scale the fluctuation amplitudes by $(\phi_k,\psi_k) = (\rho/r_n)(\hat{\phi}_k,\hat{\psi}_k)$ in order to eliminate the dominant parametric dependence on ρ/r_n as shown by the nonlinear fluid simulations of Horton, et al.[9]. We calculate the polarization factor ψ_k/ϕ_k using the linear relations in Sec. III. The anomalous particle diffusion becomes

$$\Gamma_e = -D \frac{dn_e}{dr}$$

with the electron diffusion given by

$$D = \frac{\rho}{r_n} \frac{cT_e}{eB} \alpha_e(\beta) \tag{46}$$

where the factor $\alpha_e(\beta)$ is given approximately by

$$\alpha_e = \sum_{k_o,k_\parallel} k_o^2 \left|\hat{\phi}_{k_o}\right|^2 \langle \mathrm{Im}\, \bar{g}_k^e(E,\mu)\rangle \frac{(1-\beta/\beta_c)}{(1+\beta/\beta_1)^2}$$

Here the polarization factor gives $(1+\beta/\beta_1)^{-2}$ and the critical beta β_c from ion Landau damping is estimated in Secs. 2.5 and 4.3 of Ref. 1.

We estimate that the peak of the fluctuation spectrum occurs at $\bar{k}_\parallel L_c \simeq (\beta/\beta_1)^{1/2}$ and the magnitude of $\sum|\hat{\phi}_k|^2$ and the particle-field correlation is given by $\gamma_{\bar{k}}/\omega_{\bar{k}} \simeq (m_e/m_i\beta)^{1/2}$ to obtain the final result. At long mean-free-paths, however, the quasilinear flattening of the electron velocity distribution reduces the diffusion rate[10]. The result obtained from these calculations is that

$$D = \begin{cases} \dfrac{\rho}{r_n}\dfrac{cT_e}{eB}\left(\dfrac{m_e}{m_i\beta}\right)\dfrac{(1-\beta/\beta_c)}{(1+\beta/\beta_1)^2} & \text{for } \nu_e > \nu_* \ , \\ \nu_e r_n^2\left(\dfrac{m_e}{m_i\beta}\right)^2\dfrac{(1-\beta/\beta_c)}{(1+\beta/\beta_1)^2} & \text{for } \nu_e < \nu_* \ , \end{cases} \tag{47}$$

where

$$\nu_* = \frac{c_s}{r_n}\left(\frac{\rho}{r_n}\right)^2\left(\frac{\beta m_i}{m_e}\right) .$$

For $\beta >> \beta_1$ the drift wave is transformed into the low frequency convective cell, as shown in Sec. III B, and is damped by the ion Landau resonances calculated in Sec. 4.3 of Ref. 1. Sagdeev, et al.[4] show that this low frequency hydrodynamic-like mode can be parametrically driven by higher frequency oscillations. It remains to examine this secondary mechanism for enhanced transport in the tandem mirror. The radio frequency noise that leaks into the central cell from the anisotropic plug plasma and possible lower hybrid drift wave instabilities are candidates for the parametric driving fields for the damped convective cells. Dawson has also pointed out the importance of convective cells as a mechanism for plasma transport[5].

In the case where the ion temperature gradient is stronger than the density gradient the instability is given by Eq. (31). From Eq. (23) for ψ_{k_o} and $\omega_k \sim i\gamma_k$ in Eq. (31) we find that the mode is electrostatic $|\psi_{k_o}/\phi_{k_o}| \sim \beta(1+\eta_i)/2\beta_2 < 1$ for $\beta \lesssim \beta_2 = r_n/L_c$. Quasilinear theory gives that the dominant flux is an ion thermal flux with

$$Q_i = - n_i \chi_i \frac{dT_i}{dr} \quad .$$

Fluid simulations for the related slab model ($\varepsilon_n = 0$) problem have been carried out on the CRAY as a three dimensional initial value problem[9]. The dimensionless saturation level for this instability scales as $\sum_k |\hat{\phi}_k|^2 \simeq (1+\eta_i)(2\epsilon_n)$ and the phase relation varies according to $\mathrm{Im}\,(\phi_k^* p_k) \simeq |\phi_k|^2/(1+\eta_i)^{\frac{1}{2}}(2\epsilon_n)^{\frac{1}{2}}$. Taking these formulae and the simulation results into account leads to the turbulent ion thermal conductivity

$$\chi_i = 0.3 \frac{\rho_i}{(r_n r_{pi})^{\frac{1}{2}}} \frac{cT_i}{eB} \frac{r_n}{L_t} \quad , \tag{48}$$

where $r_{pi} = r_n/(1+\eta_i)$, $(2\epsilon_n)^{\frac{1}{2}} \simeq r_n/L_t$, and the factor 0.3 is implied by the simulations. On the other hand, the small asymmetry from quadrupole magnetic fields produces[3] a thermal conductivity

$$\chi_i^{nc} = \left(\frac{r\rho_i}{L_t}\right)^2 \frac{v_i}{L_c} = \frac{\rho_i}{r_n} \frac{cT_i}{eB} \frac{r_n r^2}{L_c L_t^2}$$

in both the resonant and stochastic transport regimes. The low beta ($\beta<\beta_2$) turbulent conductivity exceeds the neoclassical conductivity by $L_c L_t/3r^2$. For high beta, however, the instability is weakened and resonant ion-wave interactions must be taken into account to determine the diffusion.

V. CONCLUSIONS

The axial drift mode eigenfunctions are analyzed for an axisymmetric model equilibrium. The mode structure and frequency are shown to change as the plasma pressure β varies from $\beta < \beta_1$ to $\beta > \beta_2$. In both regimes the axial wave equations given by Eq. (22) and Eq. (34), respectively, have turning points on the real axis in the transition region of the central cell. The polarization relations for $\psi(s)/\phi(s)$ are given in Eqs. (23) and (32). As β increases above β_1 the low beta electrostatic drift wave with frequency below $k_\parallel v_A$ transforms into a retarded Alfven wave. As the pressure increases above β_2 this mode becomes a slowly rotating convective cell with the frequency ω_k given in Eq. (39).

Taking into account the unfavorable magnetic curvature in the transition region there is a fluid-like branch of the low beta eigenmode problem. The mode rotates slowly in the ion diamagnetic direction and its growth rate is proportional to the geometric mean of the ion pressure gradient and the strength of the bad curvature. As β approaches β_2 the mode transforms into the magnetohydrodynamic mode with the finite Larmor radius terms giving rise to stable oscillations for $\omega_{*i} > \gamma_{mhd}$ as shown in Sec. III.

Taking into account the drift mode-electron resonances and the finite β mode structure derived here we analyze the problem of anomalous electron transport in Sec. IV. For a broad frequency, small amplitude fluctuation spectrum we obtain the

anomalous diffusion given in Eq. (47) for the electron drift wave turbulence. This formula shows a rapid decrease in the anomalous electron diffusion with increasing plasma pressure.

The fluid-like ion pressure gradient and curvature driven drift mode gives rise to out-of-phase potential and ion temperature fluctuations which produce an anomalous ion thermal conductivity. On the basis of quasilinear theory the anomalous ion thermal conductivity is given in Eq. (48) and scales with density, temperature, and magnetic field as the resonant-stochastic transport rate given by Kishinevskij et al.[3]. The turbulent thermal conductivity is predicted to exceed the collisional conductivity by a factor that varies with the aspect ratio of the system.

Acknowledgments

The author expresses his thanks to Drs. G. Smith, R. H. Cohen, and W. M. Nevins for their helpful criticism of the original work. He also thanks Duk-In Choi for work on various parts of the analysis. The numerical calculations were performed by Mr. Lee Leonard.

The hospitality of the Aspen Center for Physics where the work was completed is gratefully acknowledged.

This work was partially supported by the Lawrence Livermore National Laboratory and by the U.S. Department of Energy.

APPENDIX A: Electron Integral Operators

Due to the rapid bounce motion of the electrons in the mirror system compared to the drift mode frequencies the electron response in Eqs. (20), (22) and (23) contains the reactive and dissipative operators $\hat{\mathcal{L}}$ and $i\delta\hat{\mathcal{L}}$ describing the electron-drift wave coupling. Defining $s_{1,2}(E,\mu)$ as the left-hand and right-hand turning points of the electrons with energy $E = \frac{1}{2}v_{\|}^2 + \mu B(s) + \Phi(s)$ and magnetic moment $\mu = v_{\perp}^2/2B(s)$, the operators are given by

$$\hat{\mathcal{L}}\phi = \langle\bar{\phi}\rangle = 4\pi \int_0^{\infty} dE\, F_e^M(E) \int_0^{(E-\Phi)/B} \frac{d\mu B}{v_{\|}(E,\mu,s)} \frac{1}{\tau} \int_{s_1}^{s_2} \frac{ds'\phi(s')}{v_{\|}(E,\mu,s')} \qquad (A1)$$

$$i\delta\hat{\mathcal{L}}\phi = i4\pi^2 \int_0^{\infty} dE\, F_e^M(E) \int_0^{(E-\Phi)/B} \frac{d\mu B}{v_{\|}(E,\mu,s)}\, \delta(\omega-\bar{\omega}_{De}-n\omega_b) e^{in\omega_b\tau(s)} \times \int_{s_1}^{s_2} d\tau e^{-in\omega_b\tau} \phi[s(\tau)] \qquad (A2)$$

where $v_{\|} = [2(E - \mu B - \Phi)]^{1/2}$,

$$\tau(s) = \int_0^{s} \frac{ds}{v_{\|}(E,\mu,s)} \quad \text{and} \quad F_e^M(E) = (2\pi T_e)^{-3/2} \exp(-E/T_e) \,. \qquad (A3)$$

The operator $\hat{\mathcal{L}}$ averages $\phi(s)$ along the field line and has positive real eigenvalues λ between zero and unity; $\hat{\mathcal{L}}\phi = \lambda\phi$ with $0 \leqslant \lambda \leqslant 1$. The dissipative operator $i\delta\hat{\mathcal{L}}$ is treated as a perturbation to the wave equation so that we compute its effect through the flux tube volume integral as, for example, in Eq. (28). Taking the flux tube integrals of Eqs. (A1) and (A3) we obtain

$$\lambda = 4\pi \int_0^{\infty} dE\, F_e^M(E) \int_0^{E/B_c} d\mu\tau \left[\frac{1}{\tau}\int_{s_1}^{s_2} \frac{ds\phi(s)}{v_\parallel(E,\mu,s)}\right]^2 \left[\int_{-\infty}^{+\infty} \frac{ds\phi^2(s)}{B(s)}\right]^{-1} \qquad \text{(A4)}$$

$$i\delta_e = \left[\int_{-\infty}^{+\infty} \phi^*(s)\, i\delta\hat{\mathcal{L}}\phi(s)\, \frac{ds}{B(s)}\right] \left[\int_{-\infty}^{+\infty} |\phi(s)|^2\, \frac{ds}{B(s)}\right]^{-1}$$

$$= i4\pi^2\omega \sum \int_0^{\infty} dE \int_0^{E/B_c} d\mu\tau\, F_e^M(E)\, \delta(\omega-\bar{\omega}_{De}-n\omega_b)$$

$$\left|\int_{s_1}^{s_2} \frac{ds\phi(s)\exp(in\omega_b\tau(s))}{v_\parallel(E,\mu,s)}\right|^2 \times \left[\int_{-\infty}^{+\infty} |\phi(s)|^2\, \frac{ds}{B(s)}\right]^{-1}. \qquad \text{(A5)}$$

We observe that for $\phi(s)$ with odd axial symmetry $\lambda = 0$ and for $\phi(s) = \text{const}, \lambda = 1$. For $L_c \to \infty$ and $\tau = L_c/v_\parallel$ the dissipative formula for $i\delta_e$ reduces to $i\delta_e = i\pi\omega \sum_n \int dv\, F_e^M(E)\, \delta(\omega-k_\parallel v_\parallel) J_n^2(k_\parallel L_c)$ and since $\sum_n J_n^2 = 1$, the plane wave-electron resonance is recovered. In this limit the electron response is proportional to $(\omega-\omega_{ne})(1+i\delta_e)$ with $\delta_e = (\pi/2)^{1/2}(\omega/|k_\parallel|v_e)$.

APPENDIX B: Condition for Quasi-Localized Modes

In both regimes of plasma pressure the region of bad curvature can produce a partial localization of the eigenfunction. This localization or weak ballooning produces a negative eigenvalue which results in instability either through a fluid-like root or an unfavorable frequency shift depending on the parameters k_0, η_i, η_e and the magnitude of λ.

The condition for weak localization and the negative eigenvalue are derived from an analysis of

$$\phi'' + [\lambda+\hat{\varepsilon}_n(z)]\phi=0 \qquad \text{(B1)}$$

where $\hat{\varepsilon}_n(z)=-\hat{\varepsilon}_n \sin[\pi(z-L_1)/L_t]$ for $|z-L_1|\leq L_t$ and zero elsewhere. In the regime $\beta<\beta_1$ we have from Eq. (22) that

$$\lambda= \frac{\omega^2}{\varepsilon_t^2}\left(\frac{\omega-k_0}{\omega+k_0(1+\eta)} + k_0^2\right) \quad \text{and} \quad \hat{\varepsilon}_n= \frac{2k_0\omega\varepsilon_n}{\varepsilon_t^2} \quad ,$$

where $\varepsilon_t=r_n/L_t$, and for $\beta>\beta_1$ we have from Eq. (34) that

$$\lambda= \frac{\beta}{2\varepsilon_t^2}\ \omega\left[\omega+k_0(1+\eta_i)\right] \quad \text{and} \quad \hat{\varepsilon}_n= \frac{\beta\varepsilon_n p'}{2\varepsilon_t^2} \quad ,$$

where $p'=1+\eta_i+(T_e/T_i)(1+\eta_e)$.

The critical condition for quasi-localization is that that the phase of the wave function change by approximately π in the region of positive $\varepsilon_n(z)$. From Eq. (B1) we obtain

$$\int dz\sqrt{\hat{\varepsilon}_n(z)} \simeq L_t\sqrt{\hat{\varepsilon}_n} \gtrsim \pi \ . \qquad \text{(B2)}$$

When condition (B2) is satisfied there appears the first eigenvalue with $\lambda_0<0$. As condition (B2) becomes well satisfied the eigenvalue approaches $\lambda_0 \simeq -\hat{\varepsilon}_n$ and the wave is well localized. Three examples are given in Fig. 4.

For reference we give in Table AI the values of λ_0 as a function of $L_t\sqrt{\hat{\varepsilon}_n}$ for the first even and odd modes given by Eq. (B1) with $L_1 = 2L_t$. The corresponding wave functions are shown in Fig. 4.

REFERENCES

1. W. Horton, Nucl. Fusion 20, 321 (1980).
2. T.B. Kaiser, "Ballooning Stability of TMX", Lawrence Livermore Laboratory Rept. UCRL (1980).
3. M.E. Kishinevskij, P.B. Lysyanskij, D.D. Ryutov, G.V. Stupakov, B.M. Fomel', B.V. Chirikov, and G.I. Shul'zhenko, in Plasma Physics and Controlled Nuclear Fusion, (International Atomic Energy Agnecy, Vienna), Vol. II, p. 411 (1978).
4. R.Z. Sagdeev, V.D. Shapiro, and V.I. Shevchenko, [Sov. J. Plasma Phys. 4, 306 (1978)].
5. H. Okuda, C. Chu, and J.M. Dawson, Phys. Fluids 18, 243 (1975); 1762 (1975).
6. A.B. Mikhajlovskij, Plasma Instabilities in Magnetic Traps (Atomizdat, Moscow, 1978).
7. L.D. Pearlstein and J.P. Freidburg, Phys. Fluids 21, 1218 (1978).
8. W. M. Nevins (private communication, July 1980).
9. W. Horton, R.D. Estes, and D. Biskamp, Plasma Physics 22, 663 (1980).
10. A.A. Galeev and R.S. Sagdeev, in Review of Plasma Physics, edited by M.A. Leontovich, (Consultants Bureau, New York, 1979), Vol. 7, p. 103.
11. M.N. Rosenbluth (private communication).

TABLE B.I

Even Modes		Odd Modes	
$(\hat{\varepsilon}_n)^{\frac{1}{2}} L_t$	λ_0	$(\hat{\varepsilon}_n)^{\frac{1}{2}} L_t$	λ_0
1	-0.05	1	0.39-i0.27
2	-0.89	2	-0.56
3	-3.39	3	-3.32

FIGURE CAPTIONS

Fig. 1 (a) Axial variation of the magnetic strength B(s) and (b) the field line curvature driving term $\varepsilon_n(s)$ for the model axisymmetric equilibrium.

Fig. 2 (a) Local parallel wavenumber $k_{\parallel}(s)L_t$ obtained from the axial mode Eq. (22).

(b) The electron drift wave axial wave function for $k_0 = 0.6$, $\eta_i = 1$ and $\beta<\beta_1$ where $\omega r_n/c_s = 0.391$.

Fig. 3 (a) Local parallel wavenumber $k_{\parallel}(s)L_t$ obtained from the axial mode Eq. (36).

(b) The ion-drift mode and the convective cell axial wave function for $k_0 = 0.6$, $\eta_i = 1$ and $\beta>\beta_2$.

Fig. 4 The trapping of the even and odd eigenfunctions with increasing strength of the field line curvature parameter. The model equation is given in the Appendix.

Fig. 5 The frequency and the growth rate in the transitional regime obtained from the local approximation to the axial eigenvalue problem. In (a) and (b) the pressure is just below or above the onset of the magnetohydrodynamic mode in the local theory.

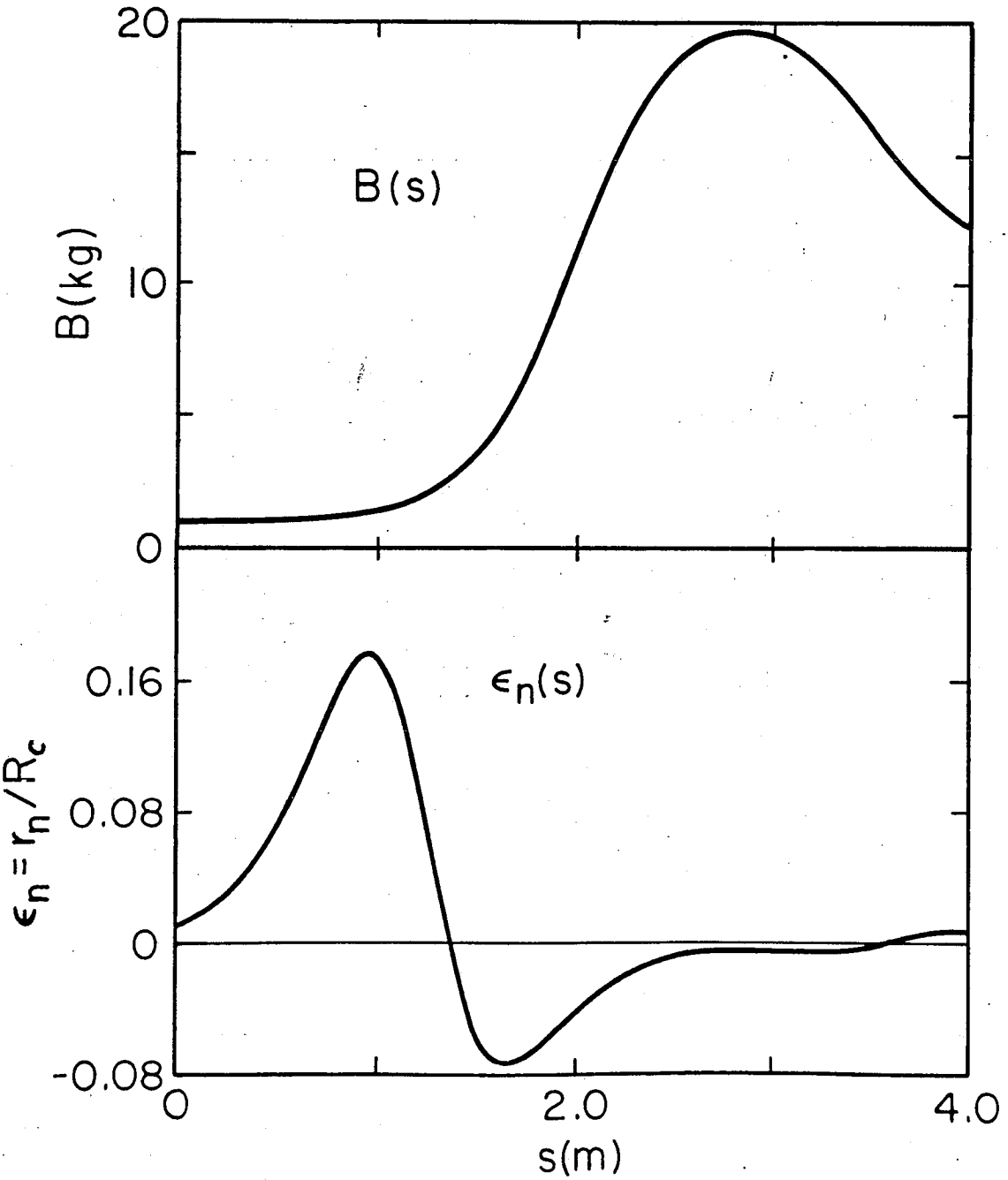

Fig. 1

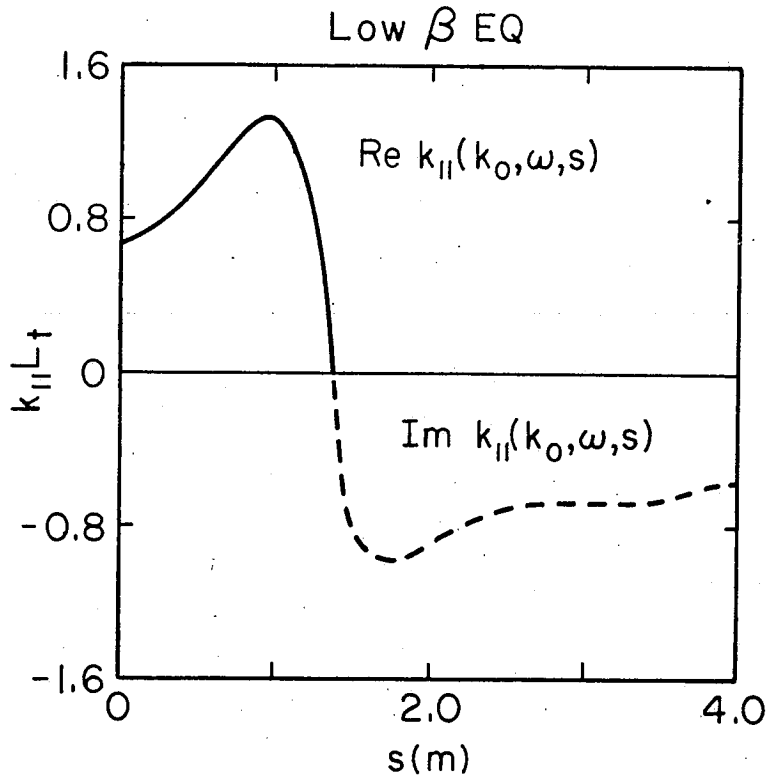
Low β EQ
1.6
0.8
0
-0.8
-1.6
$k_{||}L_t$
Re $k_{||}(k_0,\omega,s)$
Im $k_{||}(k_0,\omega,s)$
0
2.0
4.0
s(m)

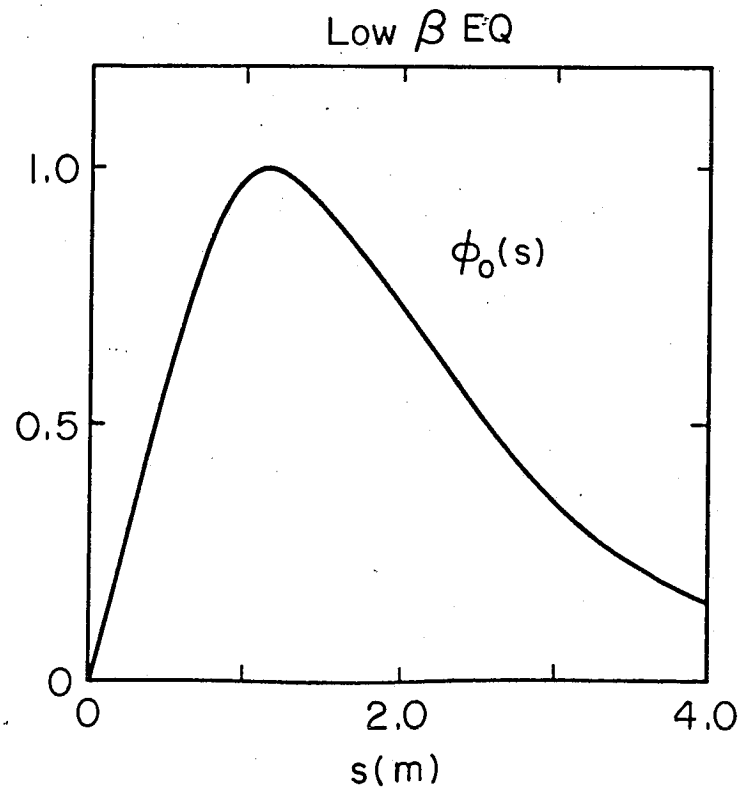
Low β EQ
1.0
0.5
0
$\phi_0(s)$
0
2.0
4.0
s(m)

Fig. 2

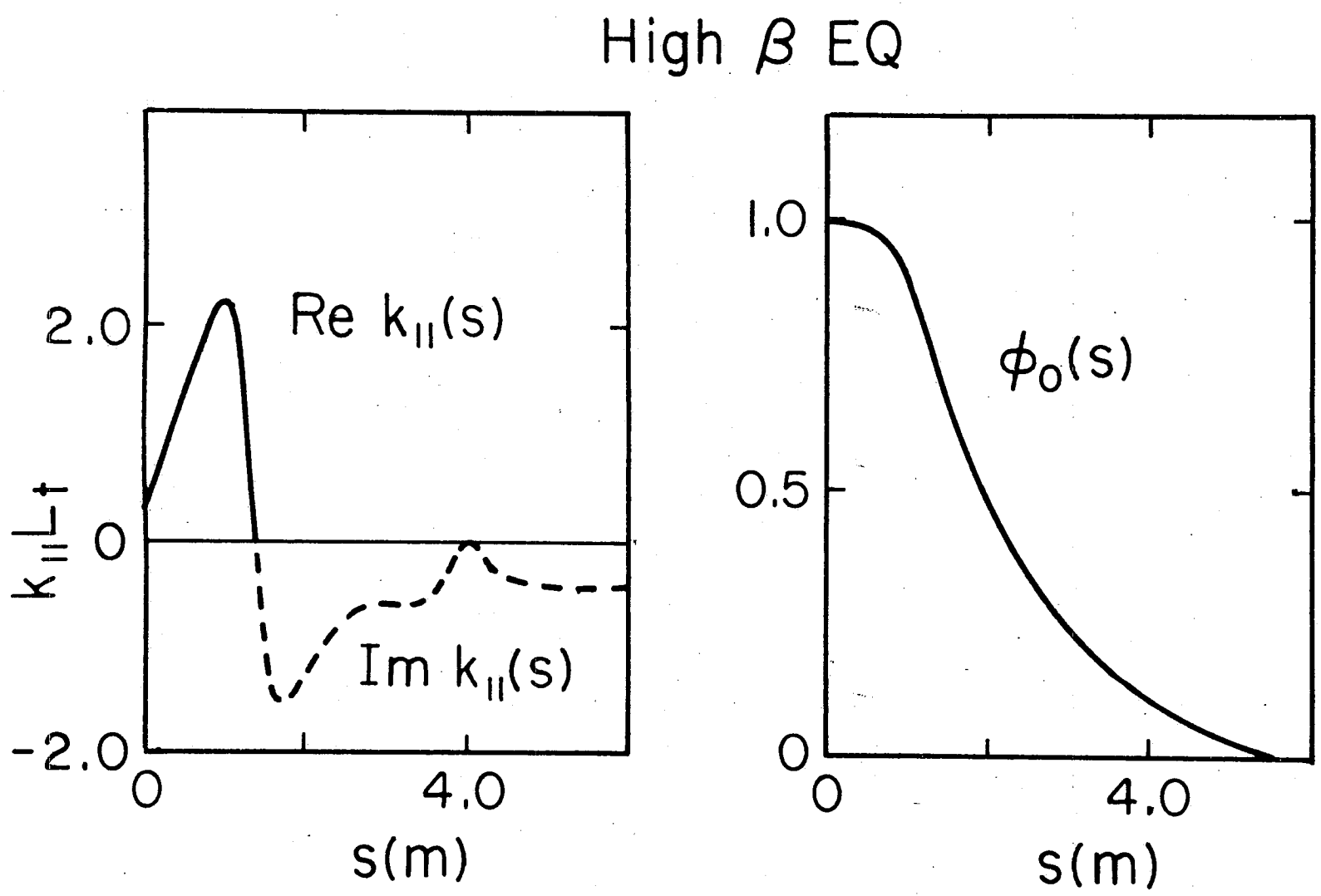

Fig. 3

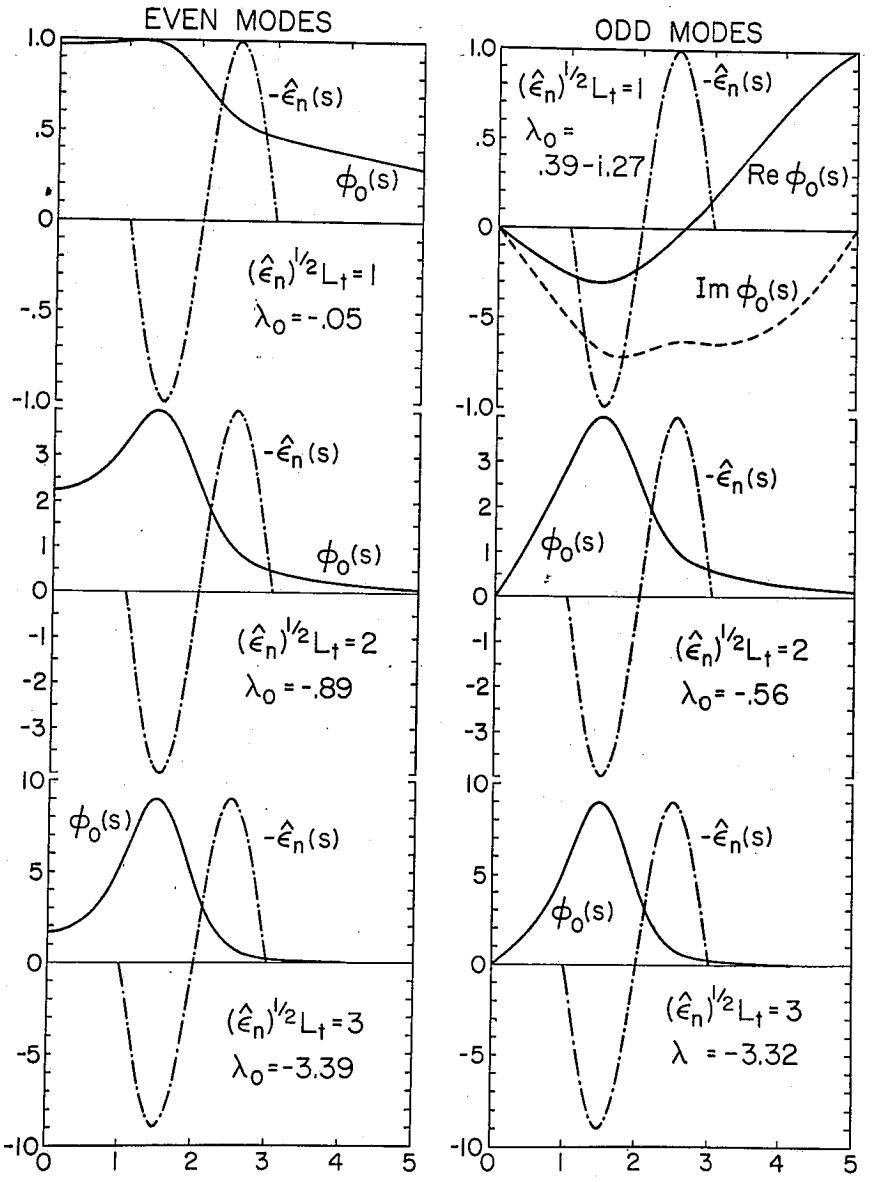
EVEN MODES
ODD MODES
$-\hat{\epsilon}_n(s)$
$\phi_0(s)$
$(\hat{\epsilon}_n)^{1/2}L_t=1$
$\lambda_0=-.05$
$(\hat{\epsilon}_n)^{1/2}L_t=2$
$\lambda_0=-.89$
$(\hat{\epsilon}_n)^{1/2}L_t=3$
$\lambda_0=-3.39$
$(\hat{\epsilon}_n)^{1/2}L_t=1$
$\lambda_0=$
.39-i.27
Re $\phi_0(s)$
Im $\phi_0(s)$
$(\hat{\epsilon}_n)^{1/2}L_t=2$
$\lambda_0=-.56$
$(\hat{\epsilon}_n)^{1/2}L_t=3$
$\lambda=-3.32$

Fig. 4

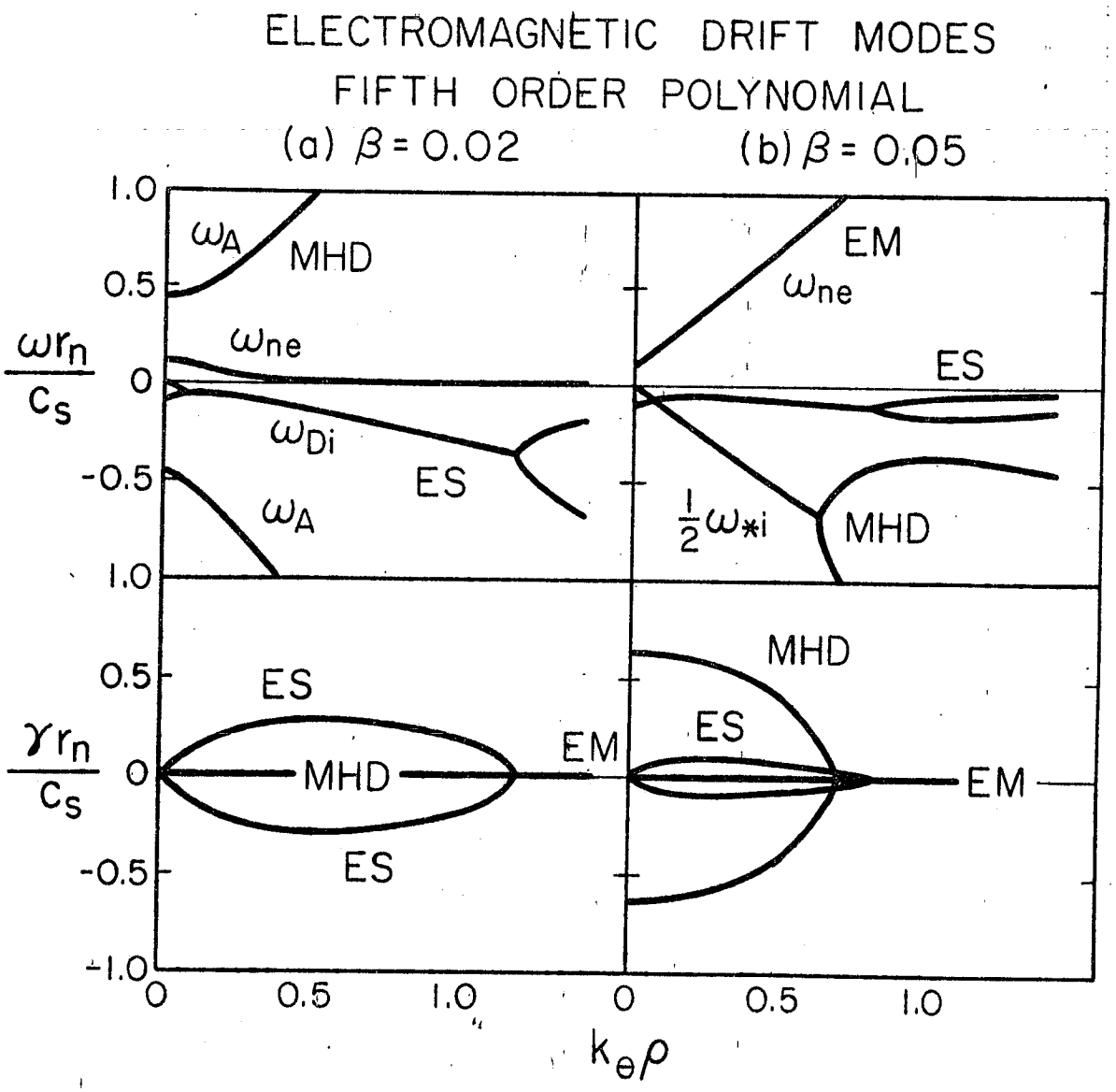
ELECTROMAGNETIC DRIFT MODES
FIFTH ORDER POLYNOMIAL
(a) β = 0.02
(b) β = 0.05
ωr_n / c_s
γr_n / c_s
ω_A
MHD
ω_ne
ω_Di
ES
EM
½ω*i
k_θρ
1.0
0.5
0
-0.5
-1.0

FIG. 5

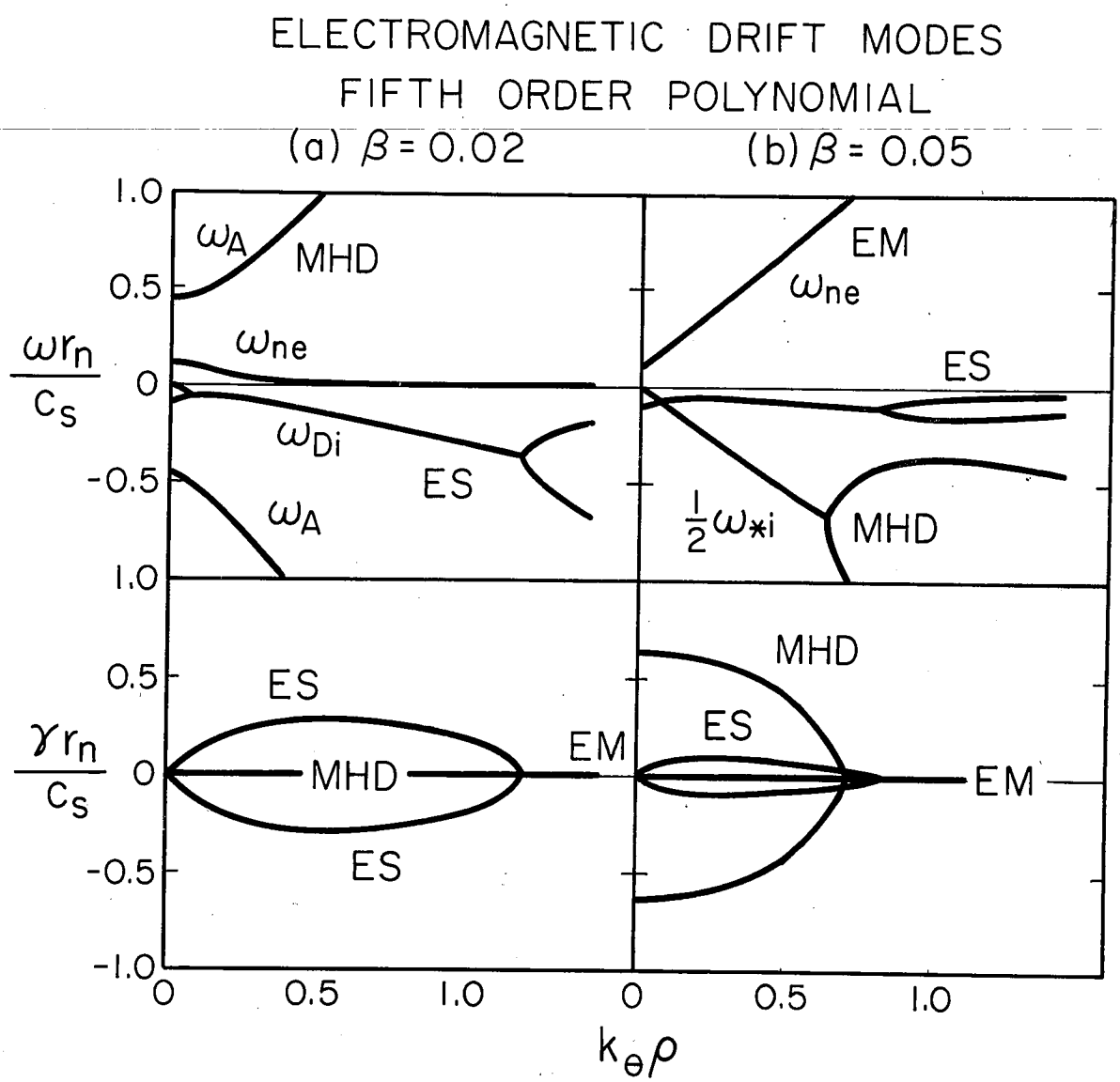
ELECTROMAGNETIC DRIFT MODES
FIFTH ORDER POLYNOMIAL
(a) β = 0.02
(b) β = 0.05
ωr_n / c_s
γr_n / c_s
ω_A
MHD
ω_ne
ω_Di
ES
EM
½ω*i
k_θρ
1.0
0.5
0
-0.5
-1.0

FIG. 5